Chemical Engineering Journal 405 (2021) 126609

Contents lists available at ScienceDirect

Chemical Engineering Journal

journal homepage: www.elsevier.com/locate/cej

Design of an overmoded resonant cavity-based reactor for ceramic matrix composites production

R. D'Ambrosio[a,b], A. Cintio[b], A. Lazzeri[a,b,c], G. Annino[b,*]

[a] Department of Civil and Industrial Engineering, University of Pisa, Via Diotisalvi, 2, 56122 Pisa, Italy
[b] Istituto per i Processi Chimico-Fisici, IPCF-CNR, Via G. Moruzzi 1, 56124 Pisa, Italy
[c] CISUP, Centro per l'Integrazione della Strumentazione dell'Università di Pisa, Lungarno Pacinotti 43, Pisa, Italy

HIGHLIGHTS

- General method for the design of overmoded resonant cavities in microwave reactors.
- Pilot-scale reactor for Chemical Vapor Infiltration of ceramic composites.
- Critical coupling conditions reached for different samples and operating conditions.
- Power dissipated in SiC_f/SiC samples exceeding 60% of the total microwave power.
- Infiltration of disc-shaped SiC_f/SiC preforms with 10 cm diameter and 1 cm height.

GRAPHICAL ABSTRACT

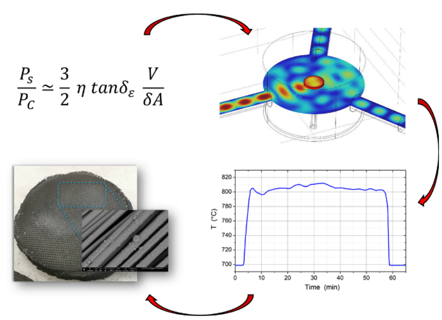

ARTICLE INFO

Keywords:
Microwave-assisted material processing
Electromagnetic resonators
Ceramic matrix composites
Chemical vapor infiltration

ABSTRACT

The use of high-quality resonant cavities in microwave-assisted reactors is highly desirable. Thanks to the low losses in the cavity walls and to the possibility to reach critical coupling conditions, high energy efficiency can indeed be achieved.

This paper describes the design, building, and test of a microwave-assisted Chemical Vapor Infiltration reactor at a pilot scale, based on an overmoded resonant cavity operating at 2.45 GHz.

First, a general design method is proposed, in which the dimensions of the cavity are chosen in order to obtain a defined mode density and a high fraction of microwave power dissipated in the sample. Among the modes of this cavity, the most efficient one for the microwave heating of the sample is then determined by means of rigorous numerical analysis.

In the graphite reactor cavity built using this approach, the condition of critical coupling is met in a large variety of samples and operating conditions. Moreover, a good agreement between experimental and simulated heating dynamics is obtained, which confirms the validity of the proposed method.

As a result, disc-shaped samples with a diameter of the order of 10 cm and a thickness of the order of 1 cm can be brought to an infiltration temperature of about 900 °C within 5 min, using a microwave power of 1000 W, with a well controllable and reproducible temperature variation. In the infiltration of Nicalon preforms, more than 60% of the microwave power is dissipated in the sample.

* Corresponding author.
E-mail address: geannino@ipcf.cnr.it (G. Annino).

https://doi.org/10.1016/j.cej.2020.126609
Received 22 April 2020; Received in revised form 18 July 2020; Accepted 9 August 2020
Available online 12 August 2020

1. Introduction

Microwave processing of materials presents great possibilities from an industrial point of view. In fact, the reduction of processing time as well as energy consumption and the improvement of material properties, which represent goals of major importance in any manufacturing process, can all be obtained thanks to the microwave heating, which is an electromagnetic energy transfer into materials with dielectric losses rather than a heat transfer. Advantages taken from microwaves as heating technique are that both the heating is volumetric, with heating speed limited only by the available microwave power, and the thermal gradients are reversed in the treated sample [1,2]. Moreover, the variability of the dielectric losses among different materials or even different phases of the same material can enable selective heating of internal or surface phases, additives or constituents, with the possibility of self–limiting reactions [3,4].

Processing of materials using high-frequency electromagnetic fields, such as microwave (MW) and radiofrequency, is gaining more and more attention at the industrial level [5]. Its potential in heating applications has been known and exploited since the early '50s, when the first MW ovens were introduced to the marketplace by Raytheon [1]. Since then, many different attempts have been made in order to broaden the range of application of MW energy, especially as an alternative heat source for materials processing. Despite some low-temperature processing applications (e.g. food, wood, rubber, polymers) have achieved industrial maturity in the '80s and are now considered as a standard production methods, MW processing has mainly remained restricted to laboratory-scale research as far as most classes of materials are concerned, in particular for high-temperature applications [6]. Successful applications of microwaves regard sintering of metals and ceramics powders [7], joining [8], waste processing [9], chemical or electrochemical reactor systems [10], composites technology [11].

A material processing technology which could highly benefit of the application of microwaves is the chemical vapor infiltration (CVI) of silicon carbide (SiC) based ceramic matrix composites (CMCs) as the SiC_f/SiC composites [12].

CMCs represent one of the latest and most promising solutions for high-temperature applications in strategic industrial sectors such as aerospace, energy and automotive [13]. In these industrial areas, materials are to be designed for severe environments, usually combining high temperatures, high-stress levels, and corrosive atmospheres. Among CMCs, SiC_f/SiC composites attract much industrial consideration for thermally loaded components such as propulsion and thermal protection systems in space applications, and refractory materials for furnaces and energy reactors [14].

Huge market opportunities are expected for CMCs provided that the major identified gaps can be overcome, such as the high cost, the difficulty of processing, and the materials reliability. New and more efficient manufacturing technologies can pave the way to improve material quality, reduce processing time, converge towards near-net-shape fabrication, trimming of spent energy, and cutting of production costs.

The CVI method is a process in which reactant gases diffuse into a porous fiber-reinforced preform and deposit a solid material, as a result of chemical reactions occurring on fiber surface, thus filling the pores inside. In the case of SiC-based CMCs, the ceramic gaseous precursor adopted is Methyltrichlorosilane, which reacts at high temperatures (900–1100 °C) in a hydrogen atmosphere to give SiC and hydrochloridric acid as a byproduct:

$$CH_3SiCl_{3(g)} \overset{H_2}{\leftrightarrow} SiC_{(s)} + 3HCl_{(g)} \quad (1)$$

This process is very slow because the movement of gas molecules is controlled by diffusion only and due to the use of relatively low pressures (100–1000 mbar) to prevent pores on preform surface from being prematurely closed. During the densification process, conditions are required for avoiding pore closure, to prevent macroscopic inter-fiber bundle pores which hamper both mechanical and thermal properties [15].

The use of MW radiation is a clean and attractive alternative due to its potential for generating a controllable inverse temperature profile during the heating of the ceramic fiber preform. In this way the reaction front of the microwave-assisted CVI process (MW-CVI) propagates from the center to the surface of the preform as its dielectric response changes. Previous works carried out by Binner [16], based on SiC_f/SiC components (5 cm diameter, 1 cm thickness), has shown that by using microwaves to enhance the CVI process, fabrication times can be reduced from hundreds of hours to around 100 h.

In the design of applicators for microwave-assisted processes, a key element is represented by the efficiency in transferring the electromagnetic energy from the source to the sample [17–21]. Ideally, such transfer should be complete, in order to guarantee the highest overall energy efficiency. However, complete absorption of the electromagnetic wave in the sample is not trivial, due to the unavoidable impedance mismatch between the wave in the propagating system and that in the sample, which causes a partial wave reflection at its surface.

The coupling of microwave radiation to the sample can be enhanced by inserting the sample inside an electromagnetic resonator. In this manner, the sample is subject to multiple passages of the wave reflected by the conductive walls of the resonator. Once the proper working conditions are found, the electromagnetic energy absorption in the sample can be maximized both by the constructive interference of the waves inside the resonator and by the destructive interference of the waves outside the resonator. In the particular case of single-port resonators, at the so-called critical coupling condition the reflected power vanishes and all the incoming power is dissipated in the resonator loaded with the sample, despite the usually low power absorption over the single passage of the wave in the sample. A detailed discussion on the effects of the multiple-wave interference in a resonator and in its excitation circuit can be found in [22,23] and in the references therein.

Whenever the critical coupling condition is reached, all the power available at the excitation port is dissipated in the resonator, partly in its walls and partly in the sample. The efficiency of the sample heating is maximized when the dielectric losses of the sample dominate over the resistive (Ohmic) losses in the resonator walls.

The use of a resonant cavity can thus provide an efficient way to control and optimize the transfer of electromagnetic energy from the source to the sample.

The microwave-assisted processes usually employ sources operating at Industrial, Scientific, and Medical (ISM) bands centered around 915 MHz, 2.45 GHz, and 5.8 GHz [24]. In general, the dimensions of a single-mode resonator are about half of the employed wavelength. Thus, a cavity operating at the frequencies of the above ISM bands can be loaded with a sample with a typical size of few centimeters. Such a solution is of modest relevance for industrial applications, where larger sample sizes are needed. Moreover, the narrow bandwidth allowed by the ISM bands would require a continuous tuning of the single-mode resonator in order to compensate for the variations of the dielectric properties of the sample with the temperature, during the heating stage, and with the density, during the processing [17].

A solution that can overcome the drawbacks of single-mode electromagnetic reactors is based on overmoded resonant cavities, having dimensions of several wavelengths. In these cavities, different modes can be simultaneously excited. The treatment of larger samples and more uniform field distributions, due to the simultaneous excitation of different modes, are benefits expected from using an overmoded reaction chamber in microwave-assisted processes [17]. The spectrum of an overmoded reactor should thus appear as a smooth, continuous distribution of electromagnetic modes. Moreover, in the cases of fixed-frequency sources, such a continuous spectrum is necessary to avoid a mismatch between the excitation frequency and the reactor operating frequencies, which change with the dielectric properties of the sample. In this regard, the possibility to achieve a sufficient level of predictability and control on the electromagnetic and thermal behaviour of overmoded reactors for the MW processing of relatively large samples was strongly questioned recently [20].

The objective of this work is to illustrate the design, building, and characterization of an efficient and well-controllable MW-CVI reactor chamber for CMCs production at a pilot scale, based on an overmoded resonant cavity operating in the 2.45 GHz ISM band and feed by magnetron sources. The reactor, enabling both MW heating and conventional heating, was built in the framework of the European project HELM [25]. This paper will focus on the core of the reactor, the reaction chamber. Further details on the whole system are provided in [26].

2. Materials and methods

2.1. Basic concepts in the design of overmoded resonant cavities

In the design of MW reactors having large dimensions with respect to the employed wavelength, a basic difficulty is the presence of several modes that can be simultaneously excited at the frequency of interest. Furthermore, the process under study is made more complex by the insertion in the cavity of the sample to process since, in general, it causes an increase in the number of modes and a mixing of them. A general analysis of the electromagnetic behavior of large MW reactors loaded by the sample to process should include a large number of variables, such as the MW frequency, the shape and the dimension of the reactor and the properties of the material forming its walls, the shape and the dimension of the sample, and its dielectric properties. In literature, this problem is usually faced assuming simple geometries for both the reactor chamber and the sample to process, in order to obtain analytic approximations for the spectral density of the modes and for the power dissipated in the sample [17].

Aim of this section is to present a general approach to the calculation of both the spectral density of the reactor and its efficiency in dissipating the electromagnetic power in samples with arbitrary shape and dielectric properties, without any assumption on the reactor shape. The only assumptions that will be made will concern the dimensions of the reactor, large enough to determine an overmoded behaviour, and the penetration depth of the radiation, which will be considered much larger or much smaller than the sample size.

In the present context, an overmoded resonant cavity can be defined as a resonant system in which consecutive electromagnetic modes overlap. This condition can be discussed on the basis of general considerations, independent of its shape. The International System of units (SI) is adopted in the formulation of the equations of this section.

Consider first the mode density $\partial(\nu)$ at the frequency ν of the electromagnetic modes of a cavity with volume V. According to the Weyl law [27], the asymptotic approximation for large frequency of the mode density is given by [28]:

$$\partial(\nu) = 8\pi V \frac{\nu^2}{c^3} \tag{2}$$

where c is the speed of light in vacuum.

The level of overlap between the modes around the frequency ν is qualitatively determined by both the average mode spacing, whose approximation is $\frac{1}{\partial(\nu)}$, and the average linewidth $\Delta\nu(\nu)$ of the resonance curves of the modes close to ν. Specifically, the property of the modal overlap can be considered to hold if the mode density is large enough that a number of modes greater than one is found in an average linewidth. Actually, the spectrum of the cavity already becomes essentially continuous whenever $\frac{1}{\partial(\nu)}$ is equal to $\Delta\nu(\nu)$. In [29], by applying a Montecarlo method, this condition is found to determine the transition from a single-mode statistics of the field distribution to a multi-mode one. Therefore, according to the definition adopted in this study, the reactor cavity can be considered as overmoded when the condition above is verified.

The average spacing between the resonance modes can be controlled by changing the volume of the cavity. At a given frequency ν, the larger the resonant cavity, the denser the mode spectrum.

The linewidth $\Delta\nu$, defining the level of the overlap between modes, can be conveniently given as the full-width at half maximum of their resonance curve.

This quantity can be expressed in terms of the quality factor Q of the resonance mode, defined as [30]

$$Q = \frac{\nu_0}{\Delta\nu} = 2\pi\nu_0 \frac{W}{P} \tag{3}$$

where ν_0 is the resonance frequency, W is the stored energy, and P is the dissipated power.

For an empty conducting cavity, the unloaded quality factor $Q_{0,C}$ of a given mode p, obtained neglecting the effect of the coupling to the excitation circuit, can be formulated as [28]:

$$Q_{0,C} = 2\frac{\iiint_V \boldsymbol{H_p} \cdot \boldsymbol{H_p^*} dV}{\delta \oiint_S \boldsymbol{H_p} \cdot \boldsymbol{H_p^*} dS} \tag{4}$$

where $\delta = \sqrt{\frac{\rho}{\pi\mu\nu}}$ is the skin depth of the electromagnetic radiation in the walls of the cavity, having a resistivity ρ and a permeability μ [31], and $\boldsymbol{H_p}$ is the magnetic field of the mode p.

A good approximation of the quality factor $Q_{0,C}$, which is independent on the cavity shape and on the specific mode, is given by [28]:

$$Q_{0,C} \simeq \frac{3}{2}\frac{V}{\delta A} \tag{5}$$

where A is the surface area of the cavity. The basic assumption behind (5) is that the electromagnetic fields are uniformly distributed in the reactor cavity, except close to its boundaries. A more accurate determination of the average value of the quality factor $Q_{0,C}$ of an ovemoded cavity can be found in [32,33], in which this quantity is obtained with a statistical approach developed for reverberation chambers.

According to (2) and (5), the knowledge of volume, surface area, and resistivity of a conductive cavity enables the estimation of the mode overlap at a given frequency, under the adopted condition of overmoded cavity. This condition can be expressed as a relationship between the wavelength λ of the electromagnetic radiation and the volume δA related to the skin depth:

$$\lambda^3 \simeq \frac{16}{3}\pi\delta A \tag{6}$$

The increase of the cavity surface area A above the value provided by (6) reinforces the overlap between modes. However, in general this option is not convenient for the energy efficiency.

To elucidate this point, consider a reactor loaded with a sample of volume V_s which is to be processed. The microwave power P coupled to the reactor is now partially dissipated in the walls of the reactor (P_C) and partially in the sample (P_s):

$$P = P_C + P_s \tag{7}$$

Equation (7) can be reformulated in terms of quality factors taking into account the second part of (3), as

$$\frac{1}{Q_0} = \frac{1}{Q_{0,C}} + \frac{1}{Q_{0,s}} \tag{8}$$

where Q_0 is the total unloaded quality factor of the cavity and $Q_{0,s}$ is the unloaded quality factor of the cavity which is calculated taking into account only the dielectric losses in the sample. The latter is given by the relation

$$\frac{1}{Q_{0,s}} = \eta\ tan\delta_\varepsilon. \tag{9}$$

where the loss factor $tan\delta_\varepsilon = \frac{\varepsilon''}{\varepsilon'}$ is the ratio between the imaginary and real part of the dielectric permittivity ε of the sample, $\varepsilon = \varepsilon^{'} - i * \varepsilon^{''} = \varepsilon_0(\varepsilon_r^{'} - i * \varepsilon_r^{''})$, ε_0 is the permittivity of free space, and the pedix r indicates the components of the relative permittivity ε_r [29]. The electric energy filling factor

$$\eta = \frac{\iiint_{V_s} \varepsilon' \boldsymbol{E_p} \bullet \boldsymbol{E_p^*} dV}{\iiint_V \varepsilon' \boldsymbol{E_p} \bullet \boldsymbol{E_p^*} dV} \tag{10}$$

represents the fraction of electric energy stored in the sample.

In the same spirit of the approximation leading from (4) to (5), let us assume that the electric energy is distributed in a substantially uniform way in the reactor loaded with the sample. The physical basis of this assumption can be found in the discussions presented in [34]. The condition of constant electric energy density requires, in particular, that the penetration depth of the radiation in the sample is larger than its dimensions. In this case, the electric energy filling factor η can be simply expressed as:

$$\eta \approx \frac{V_s}{V} \tag{11}$$

From the point of view of the MW-assisted process, the microwave power dissipated in the walls of the reactor due to ohmic losses represents a reduction in efficiency and should be minimized, in favor of the power dissipated in the sample. From (5) to (11), one can obtain the ratio between P_s and P_C:

$$\frac{P_s}{P_C} \simeq \frac{3}{2}\eta\, tan\delta_\varepsilon \frac{V}{\delta A} \approx \frac{3}{2} tan\delta_\varepsilon \frac{V_s}{\delta A}. \tag{12}$$

The combination of (7) and (12) enables the determination of the fraction of power dissipated in the sample, which can be written as:

$$\frac{P_s}{P} = \frac{1}{1 + \frac{P_C}{P_s}} \approx \frac{1}{1 + \frac{2\,\delta A}{3\, tan\delta_\varepsilon V_s}}. \tag{13}$$

Finally, from (12) it can be concluded that an increase in the surface area of the reactor cavity results in a decrease in the efficiency of the microwave heating of the sample, given the characteristics of the materials constituting the cavity and the sample to process. Accordingly, the surface and, ultimately, the volume of the reactor cavity must be set to the minimum value compatible with the other constraints, in the considered case that one of overmoded structure.

A similar conclusion holds for conducting samples. In the case in which the skin depth in the sample, δ_s, is much smaller than the minimum sample dimension, the ratio between P_s and P_C is given by

$$\frac{P_s}{P_C} \simeq \frac{\delta_s A_s}{\delta A} \tag{14}$$

where A_s is the sample surface area.

In general, the accuracy in the determination of the ratio $\frac{P_s}{P_C} \simeq \frac{3}{2}\eta tan\delta_\varepsilon \frac{V}{\delta A}$ is strongly related to the accuracy in the determination of the filling factor η. In specific cases, an exact calculation of η is possible, as discussed for instance in [17,35].

Finally, (12) and (14) provide a quick way to assess how effectively the MW power is used and thus to decide the convenience of the microwave heating of a given sample. Together with (6), they represent a *vademecum* in the design of overmoded cavities of general shape for the MW-assisted processing of arbitrary samples, formulated for the first time to the best of our knowledge.

2.2. Materials of interest and dimensions of the reaction chamber

The quantities playing a key role in the design of an efficient microwave reactor chamber with overmoded behavior are those defining (6), (12), and (14).

In the case here considered, the microwave frequency is 2.45 GHz and the typical sample to be infiltrated with the MW-CVI technique is a preform based on polycarbosilane-derived Si–C–O Nicalon NL-202 fibers (Nippon Carbon, Tokyo, Japan), with minimum dimensions of about 10 cm in diameter and 1 cm in thickness. The determination of the most convenient dimensions of the reactor chamber requires the knowledge of both the dielectric properties of the sample and the resistivity of the chamber walls.

The dielectric properties as a function of the temperature T of different Nicalon preforms were determined using a rigorous measurement technique [36], whose detailed description will be published elsewhere. Fig. 1 shows the results of the measurements from room T to the usual infiltration temperature of 900 °C.

Another essential point in the building of the reactor cavity is the choice of the material forming its walls, given the conditions it must satisfy. In particular, the electric resistivity of this material must be low to reduce the Ohmic losses in the cavity walls to a level well below the dielectric losses in the sample. Moreover, it must be chemically inert to operate for a long time in a chemically aggressive environment, characterized by a very hot sample and highly reactive chemical species. Finally, its resistivity must remain low enough after many infiltration cycles.

A material that displays these properties is graphite, in particular the FP2584-grade graphite produced by SKT [38]. The choice of the most suited graphite grade was made after a direct determination of its microwave resistivity, obtained with a modified version of the Courtney method [39]. In this technique, a microwave resonator consists of a low-loss dielectric disc inserted between two metallic plates. Usually, the dielectric properties of the disc can be obtained from the resonance frequency and the quality factor of the resonant system provided that the resistivity of the plates is well known. However, this setup can also be employed to measure the effective microwave resistivity of the

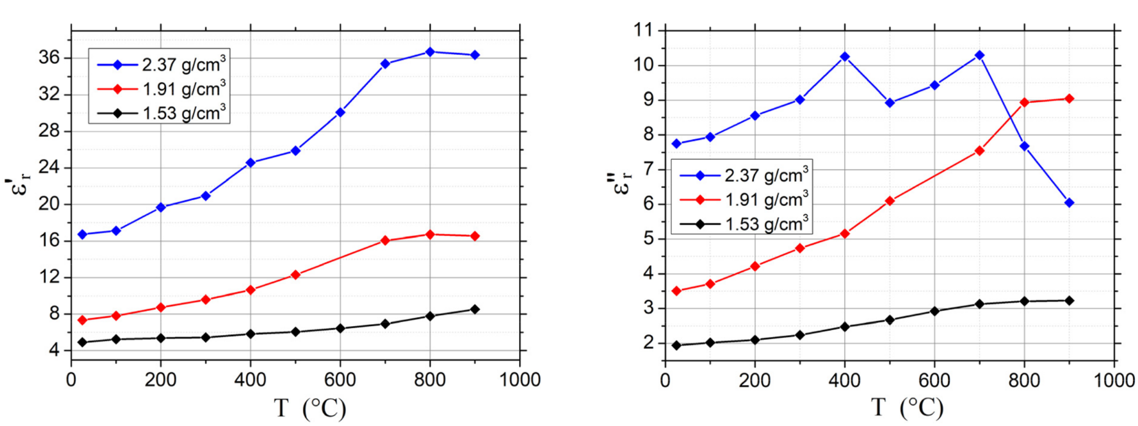

Fig. 1. Relative dielectric permittivity of polycarbosilane-derived Si–C–O Nicalon NL-202 preforms measured at different temperatures and infiltration levels. Left: real part of the permittivity. Right: imaginary part of the permittivity. The samples were provided by ATL [37].

plates whenever the dielectric properties of the disc are known.

According to the results of these measurements, the microwave resistivity of the FP2584-grade graphite at room T is 1400 ± 1 μΩ*cm. The resistivity of the reactor walls is expected to decrease to about 1000 μΩ*cm during an infiltration run, when the walls reach temperatures between 200 °C and 300 °C [40].

It is now possible to define the reactor chamber shape and its volume, given all the other quantities involved in (6) and (12). For the sake of simplicity in the manufacturing, a cylindrical geometry was considered, with a diameter of the order of 50 cm and a height of the order of 30 cm. The choice of an elongated cross-section for the cavity depends on the predominant interest in processing flat samples, whose lateral dimensions are much larger than the thickness.

In the given setup, around 2.45 GHz the typical distance between consecutive resonant modes is of the order of 3 MHz, and their typical full-width at half maximum is 0.8 MHz. The insertion of the sample leads to an additional broadening of the resonance lines, owing to the dielectric losses introduced by the sample. This broadening is at least of factor 2, since the target is to have at least 50% of the power dissipated in the sample. A further broadening of the resonance lines is due to the coupling of the cavity to the excitation circuit propagating the microwave radiation. The linewidth of the resonance mode at the critical coupling is double to that at low coupling levels, at which the unloaded quality factor is calculated [17].

Taking into account both the presence of the sample and the critical coupling to the external microwave circuit, the proposed graphite cavity behaves as an overmoded resonator around 2.45 GHz. In the system composed by the graphite cavity and the 1.53 g/cm^3 Nicalon sample of Fig. 1, the ratio P_S/P_C is expected to be 1.67 at the beginning of the microwave heating process, so about 63% of the electromagnetic power coupled to the reactor is dissipated in the sample and about 37% in the reactor walls, as calculated from the second part of (12) and (13). At the critical coupling, the above fractions refer to the total microwave power reaching the reactor.

For the considered sample, a good microwave heating efficiency is thus expected with the proposed MW-CVI reactor. In general, the energy efficiency of the reactor is expected to increase with the volume of the sample thanks to the increase of the filling factor, provided that the critical coupling condition is still fulfilled.

The above results were obtained with the help of a general approach essentially based on the assumption that the electric energy is equally distributed in the volume of the reactor chamber. A more detailed analysis of the actual electromagnetic fields in the cavity, as well as of the resulting efficiency and temperature profile in the sample, requires a rigorous numerical modeling of the reactor, both empty and loaded with sample and sample holder. The aim of the next section is to illustrate this analysis and to present the room temperature tests of the reactor. All the numerical results are based on the Comsol Multiphysics software [41].

3. Results and discussion

3.1. Reactor chamber design and room temperature tests

The final structure adopted for the reactor chamber is shown in Fig. 2. It is composed of a cylindrical cavity with a diameter D of 49.35 cm and a height H of 30.6 cm. The microwave radiation can enter the cavity through three identical circular waveguides oriented at 120° to each other and placed in the horizontal median plane of the cavity. Each waveguide is cylindrical with an inner diameter of 9 cm and a length of 27.5 cm and is made by the same graphite material forming the chamber. The waveguides are connected to the electromagnetic sources by means of WR340 rectangular waveguides made of aluminum. A system of moving stubs mounted in a magic T tuner is inserted in each excitation channel, with the aim of controlling and adjusting the coupling level until a nearly critical coupling level is reached. In the heating and infiltration tests, a normalized reflected power lower than −20 dB was considered equivalent to the critical coupling level for all practical purposes.

The main reason behind the choice to excite the reactor by means of different waveguides is the flexibility of use. Switching from one sample to another characterized by different shapes, sizes, and dielectric properties can require very different levels of MW power to reach the desired infiltration temperature, possibly exceeding the maximum power delivered by a single magnetron. Moreover, the combination of several, lower power sources instead of a single source of high power is advantageous in terms of reduced risk of sparks or plasma generation in the excitation channel. In addition, the concurrent use of different excitation ports enables, in general, a better heating uniformity.

In the lower part of the chamber, a movable graphite plate is inserted with the purpose of providing a frequency tuning of the resonance modes. This element is necessary in order to match the frequency of the mode of interest with that of the magnetron source, which is fixed. The movable plate is a disc with 47.35 cm diameter and 1 cm thickness, coaxial to the cylindrical chamber and placed at about 0.6 cm from its base. Inlet and outlet gas connections were included in the modeling.

The typical resonance spectrum calculated for the empty reactor excited through one of the three channels is shown in Fig. 3, for a frequency interval corresponding to the ISM band centered around 2.45 GHz. In the simulations, the passive channels were terminated by a short circuit. Among the many modes that can resonate in this interval, the coupling system is efficient in transferring energy to those around 2.441 GHz, 2.45 GHz, and 2.475 GHz. The electric field of these modes, in some representative planes of the reactor, is shown in the insets of Fig. 3.

According to the electric field distribution, the mode with the highest electric energy in the central part of the reactor cavity, where the sample will be placed, is that resonating at 2.475 GHz.

A graphite chamber was built following the design of Fig. 2. Its electromagnetic spectrum was determined by means of a vector network analyzer, connected to the microwave channel of interest by means of a coaxial cable-to-waveguide transition. In the measurement of the S_{11} parameter of the reactor, the stubs on the passive channels were adjusted in order to have a short-circuit condition. The reference level in the determination of S_{11} was obtained short-circuiting the end of the coaxial cable-to-waveguide transition.

The experimental and the simulated spectra of this cavity are reported in Fig. 4, for frequencies around the 2.475 GHz mode, together with the spectrum of a magnetron source feeding the reactor. The latter was determined by means of electromagnetic compatibility techniques. Fig. 4 shows a good agreement between the modeling and the experimental results. The close matching between the resonance frequency of the 2.475 GHz mode and the main emission peak of the magnetron was obtained with proper positioning of the movable graphite plate.

Another important element in the practical use of the reactor is the sample holder, whose function is to keep the sample in the most convenient position inside the reactor cavity. The material forming the sample holder must be again inert with respect to the extremely reactive environment in which it is placed. Moreover, it must be as much as possible transparent to microwaves, so as to prevent absorption of a significant fraction of the microwave power, which could be detrimental both for its chemical stability and for the efficiency of the infiltration process. A material that was proved compatible with these conditions is a low-loss grade fused quartz (Momentive 214 [42]), whose relative permittivity at the infiltration temperature is about ε_r^{qtz} = 3.81-i*0.001, as measured.

A 'chair-like' geometry was adopted for the sample holder, as shown in the inset of Fig. 5. In the infiltration processes, a disc of aluminosilicate fiberboard (Duraboard 1600 [43]), with 10 cm diameter and 1 cm thickness, is usually inserted between the sample holder and the sample, in order to avoid local damage of the latter due to the direct

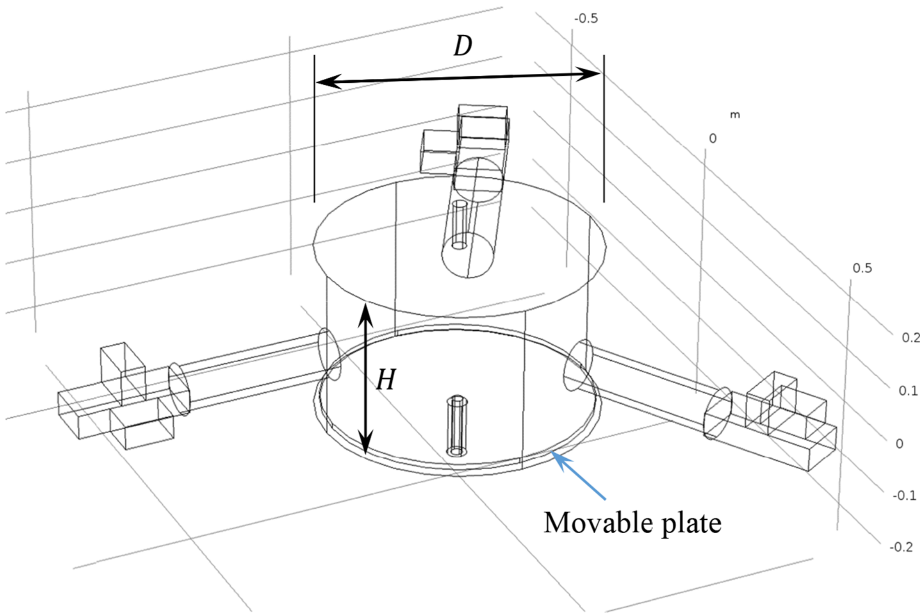

Fig. 2. 3D view of the inner cavity of the reactor, including the excitation waveguides and the gas connections. The diameter *D* and the height *H* of the cavity are indicated, as well as with the movable plate.

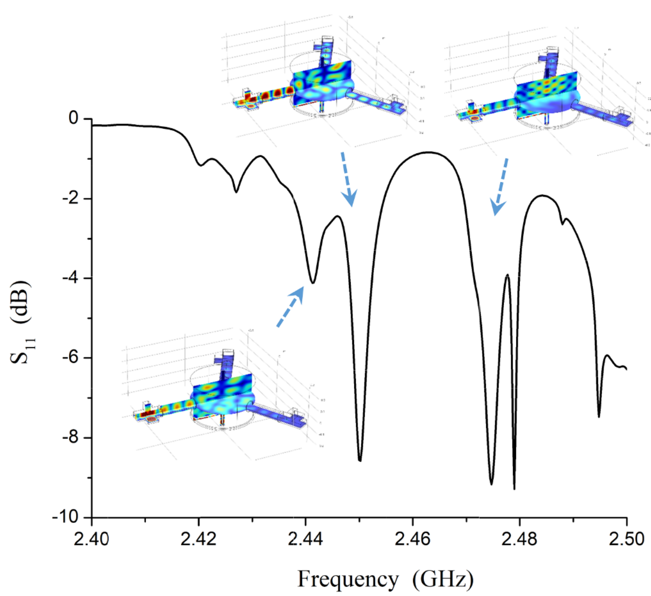

Fig. 3. S_{11} parameter of the electromagnetic signal reflected by the cavity shown in Fig. 2, excited through the waveguide on the left of the figure. Data obtained from numerical modeling. The coupling level was not optimized, as the main objective was to determine the frequency of the resonance modes. From left to right, the insets show the electric field distribution for the modes resonating at 2.441 GHz, 2.45 GHz, and 2.475 GHz, respectively.

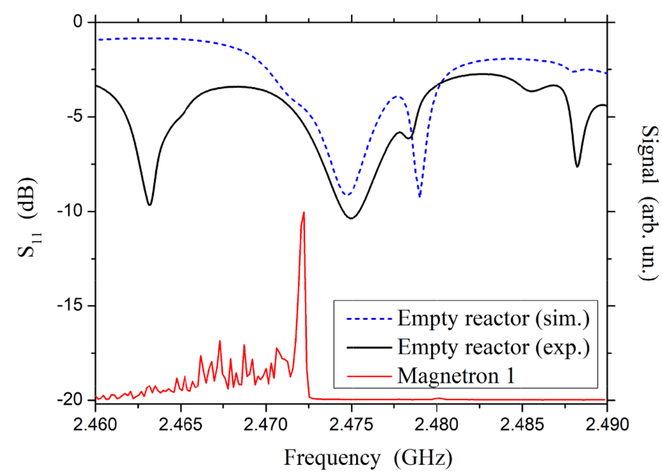

Fig. 4. Comparison between the experimental spectrum of the graphite chamber built following the design of Fig. 2 and its simulated spectrum (left y axis). In the determination of the experimental spectrum of the empty cavity, the coupling level was not optimized. The spectrum of a magnetron source exciting the reactor, with amplitude and baseline arbitrarily normalized, is also shown (right y axis).

contact with sample holder columns. Moreover, the Duraboard disc reduces the thermal irradiation of the sample, which is thus subject to a slower cooling.

The dielectric permittivity of Duraboard at the infiltration temperature resulted about ε_r^{Dur} = 1.45 – i*0.009. Thanks to the high porosity and low dielectric losses, the Duraboard disc does not interfere significantly either with the microwave heating and with the flow of the reactant gases.

The effects of the quartz sample holder and the Duraboard disc on the experimental spectrum of the reactor is shown in Fig. 5. As expected, the position and the coupling of the resonance mode are weakly modified by the presence of these elements, characterized by small volume and relatively low dielectric permittivity.

The experimental spectrum of the reactor loaded with a 1.53 g/cm^3 Nicalon disc with 10 cm diameter and 1 cm thickness, placed on top of the sample holder plus the Duraboard disc, is shown in Fig. 6, together with the spectrum of the magnetron.

The insertion of the Nicalon sample in the reactor gives rise to only a small shift in the resonance frequency of the mode of interest, which remains well superposed to the magnetron emission. Such behavior is common to several other materials of interest, as shown by Fig. 7, which reports the spectrum of the reactor loaded with similar disc-shaped specimens made of Tyranno ZMI fibers and carbon fiber cloth. The Tyranno ZMI fiber-based preform was coated with a pyrolytic carbon coating (thickness of 100 nm) and densified through conventional CVI from 1.008 g/cm^3 up to 1.298 g/cm^3.

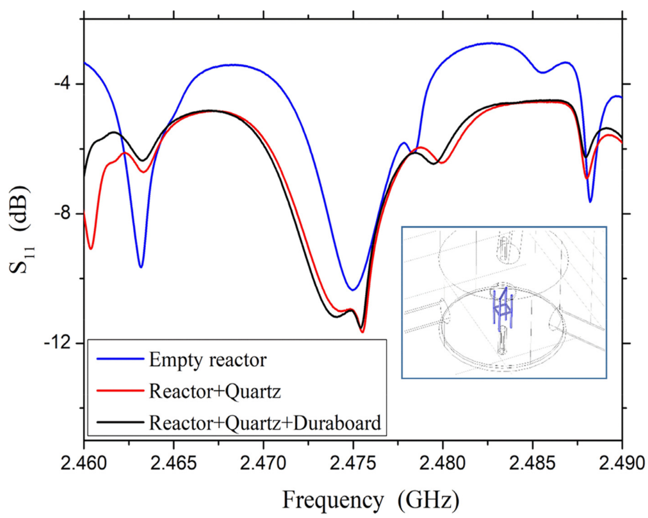

Fig. 5. Comparison among the experimental spectrum of the empty reactor chamber, the spectrum of the reactor loaded with the quartz sample holder, and the spectrum of the reactor loaded with both the quartz sample holder and the Duraboard disc. The inset shows the typical arrangement of the quartz sample holder (shaded region) and of the Duraboard disc.

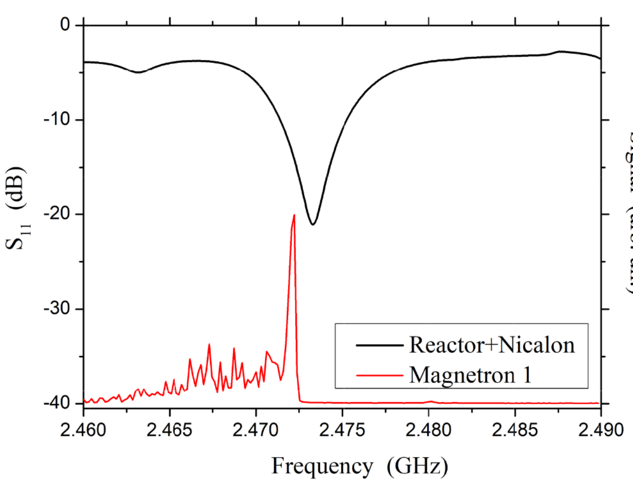

Fig. 6. Experimental spectrum of the reactor loaded with the quartz sample holder, the Duraboard disc, and a Nicalon disc (left y axis), together with the spectrum of a magnetron source exciting the reactor (right y axis). Both the Duraboard disc and the Nicalon disc have a diameter of about 10 cm and a thickness of 1 cm.

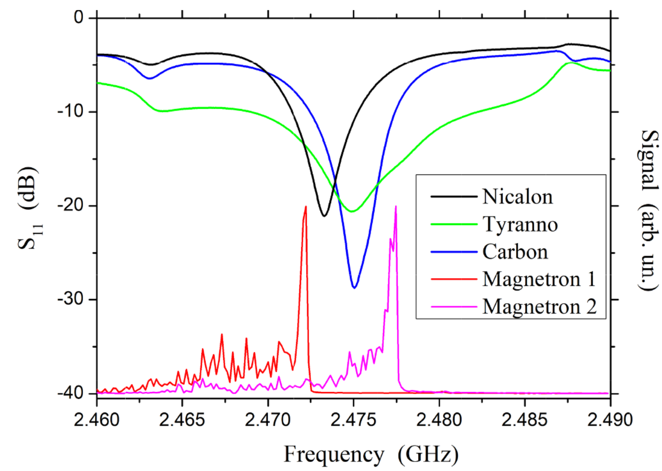

Fig. 7. Comparison among the experimental spectra of the reactor loaded with a Nicalon sample, with a Tyranno ZMI fibers sample, and with a carbon fibers cloth sample (left y axis), all placed on the quartz sample holder and the Duraboard disc. The spectra of two of the available magnetron sources, with amplitude and baseline arbitrarily normalized, are also shown (right y axis).

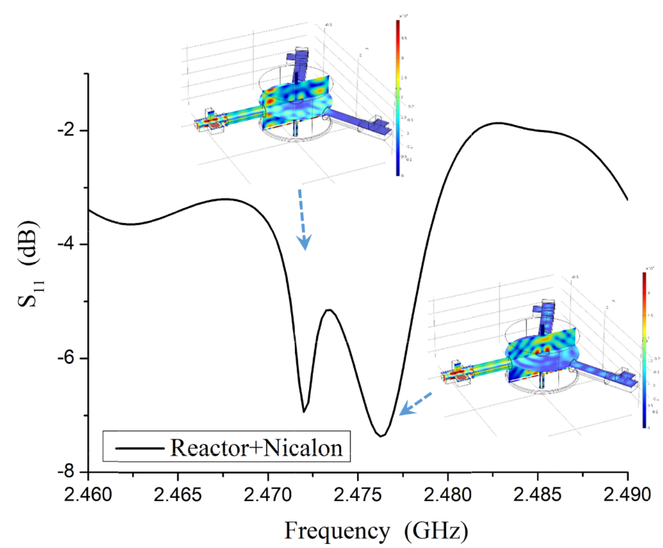

Fig. 8. Calculated resonance spectrum of the reactor loaded with the quartz sample holder, the Duraboard disc, and a Nicalon disc. The position of the stubs was not optimized. From left to right, the insets show the electric field distribution for the modes resonating at 2.472 GHz and 2.4763 GHz, respectively.

The Tyranno fiber sample is representative of high dielectric loss materials, whereas the carbon fiber sample is representative of conducting materials. For all the materials considered in Fig. 7, the resonance mode of interest is always well coupled and only slightly shifted with respect to the empty reactor case. In general, a sample that is small with respect to the resonant system in which is inserted leads to a small frequency shift of the resonance mode, owing to its small filling factor [44,45].

The frequency detuning introduced by different samples can be overcome either by using a second available magnetron emitting at a higher frequency, as shown in Fig. 7, alone or in combination with the first magnetron, or by acting on the movable plate. In the infiltration tests conducted so far, all the investigated samples were processed by using one of the two magnetrons indicated in Fig. 7, without the need to adjust the position of the movable plate.

As shown by Fig. 7, the coupling level achievable with the investigated samples can easily be brought below −20 dB at the emission of one of the two magnetrons by optimizing the position of the tuning stubs. Accordingly, in practice all the microwave power reaching the reactor can be transferred to its electromagnetic modes.

The 1.53 g/cm^3 Nicalon sample will be taken as a reference in the following. The room temperature spectrum of the reactor loaded with the Nicalon sample is shown in Fig. 8.

Two main modes are visible in Fig. 8, one resonating at 2.472 GHz and one resonating at 2.4763 GHz. The distribution of the electric field of these modes is shown in the insets of the figure. The mode at 2.472 GHz corresponds to a ‘surface’, Whispering Gallery-like mode [46], in which the electromagnetic energy is prevalently confined around the surface of the cavity. On the contrary, the mode at 2.4763 GHz corresponds to the ‘volume’ mode of interest, in which the electromagnetic energy is more evenly distributed in the entire volume of the cavity, in particular in its center, where the sample is placed. The slight discrepancy between the calculated (2.4763 GHz) and the experimental (2.473 GHz) resonance frequency of the volume mode is mainly due to the irregular shape of the sample.

In the design of the reactor, care must be taken to avoid coupling to

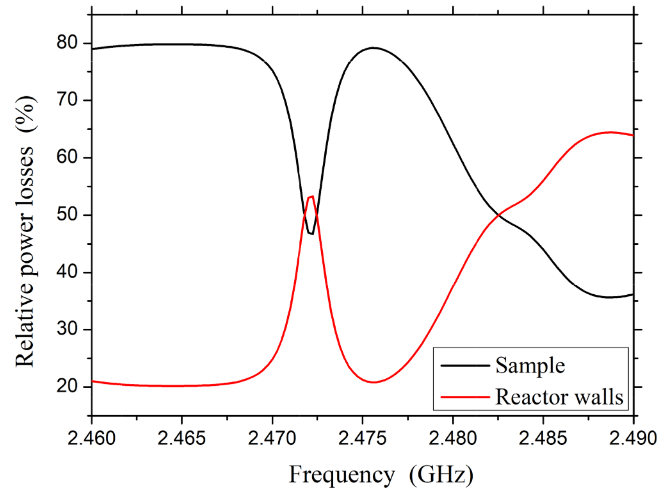

Fig. 9. Calculated fraction of microwave power dissipated in the sample and in the walls of the reactor, in the case of reactor loaded with the quartz sample holder, the Duraboard disc, and a Nicalon disc (see also Fig. 8).

the surface modes, which make problematic the heating of samples placed in the center of the reactor chamber. This aspect is evidenced by the fraction of power dissipated in the sample (P_s/P) and by that in the walls of the reactor (P_C/P), both reported in Fig. 9. For the surface mode, the majority of the microwave power is dissipated in the walls of the reactor. On the contrary, for the mode of interest the 80% of the power coupled to the reactor is dissipated in the sample. This value can be compared with the value provided by the second part of (13), given by 54% taking now into account the extra surface introduced by the movable plate. Despite the simplicity of the analysis leading to (13), the agreement between the approximate and the rigorous result is still acceptable. A similar agreement has been verified under very different conditions.

Through the many infiltration cycles conducted so far, the efficiency of the reactor cavity was continuously monitored to check for a possible deterioration of its characteristics, in particular the resistivity of the graphite walls. This quantity can be directly obtained from the quality factor of a reference resonance mode, according to (4). After a marked increase with the initial infiltration processes, the resistivity of the graphite walls stabilized to about 4000 μΩ*cm at the typical temperatures of the reaction chamber. The fraction of microwave power currently dissipated in the reference Nicalon sample is $P_s/P \approx 62\%$.

3.2. Microwave heating and infiltration tests

In stationary conditions, all the microwave power absorbed by the sample through its dielectric losses is dissipated as heat, assuming no chemical reactions. Under the conditions of high temperatures and low pressures at which the infiltration reactions are usually conducted, the dominant dissipation mechanism is given by the thermal irradiation towards the much colder walls of the reactor. Accordingly, the microwave power P_h necessary to keep the sample at the infiltration temperature T can be estimated by means of the Stefan-Boltzmann law

$$P_h = \epsilon \sigma A_s T^4 \qquad (15)$$

where $\sigma = 5.67{*}10^{-8}$ W m^{-2} K^{-4} is the Stefan-Boltzmann constant, ϵ is the emissivity of the sample, A_s its surface area, and T the surface temperature in Kelvin degrees.

Under the assumption that the sample is homogeneously heated, $\epsilon \approx 1$, and neglecting the thermal irradiation towards the Duraboard disc, the power necessary to heat the reference Nicalon sample to 900 °C is about $P_h = 1200$ W.

In real process conditions, the spatial variation of the electric field in the sample volume and the limited thermal conductivity of most ceramic materials lead to an inhomogeneous sample heating, characterized by localized domains with much higher temperature (hot spots). The actual temperature distribution of the sample can be calculated by means of a multiphysics numerical modeling, in which the coupled electromagnetic and thermal problems are solved simultaneously and in a self-consistent way.

The accuracy of the multiphysics models describing the reactor loaded with the sample was first assessed comparing the power P_h obtained from (15) with the numerically obtained value, in the same conditions of very high thermal conductivity and thermal emission from the free surfaces of the sample. In the case of the numerical model, the power P_h was directly determined as the microwave power released in the sample. The discrepancy between these calculations resulted lower than 1%.

The preparation of realistic multiphysics models requires the knowledge, as functions of T, of the dielectric permittivity, the specific heat, the thermal conductivity, and the emissivity of the sample. For the materials of interest, all these quantities were determined in the framework of the project HELM.

In the case of the reference Nicalon sample, a multiphysics model was prepared with the aim of determining the sample heating dynamic and the temperature distribution in the typical infiltration conditions. The microwave frequency was set to 2.4763 GHz, corresponding to the volume mode of Fig. 8. The microwave power coupled to the reactor was fixed to 1000 W at the beginning of the microwave heating process, in which the temperature of the reactor walls and that of the sample was set to 200 °C. The dielectric and thermal quantities employed in the multiphysics model are reported in the Supplementary data associated with this article. In stationary conditions, the resulting temperature distribution on the surface of the sample is shown in Fig. 10.

The evolution of the Nicalon temperature, determined at the hotspot on the upper surface of the sample, is reported in Fig. 11. The characteristic time of the nearly exponential curve describing the sample heating is of the order of 2 min.

More information on the temperature of the sample and on the electromagnetic field in the reactor during the heating process, both obtained from the multiphysics model, is provided by two movies reported as Supplementary data in the online version of this article. The first movie (Sample heating.gif) shows the temperature of the upper surface of the sample during the first 500 s of the microwave heating. At the end of this period, the sample temperature is close to its stationary value. In addition to the sample temperature, the second movie (Sample heating and electric field.gif) reports the norm of the electric field in a horizontal plane close to the sample. The increase of the temperature from 200 °C to above 800 °C corresponds to a strong variation of the dielectric properties of the sample, according to Fig. 1. This variation reflects on the electromagnetic fields in the reactor. However, the second movie shows that there is just a small rearrangement of the electric field distribution during the sample heating. This fact confirms the robustness of the electromagnetic response of the reactor with respect to the dielectric properties of the sample, which was already evidenced by the curves of Fig. 7, demonstrating that a stable and controllable electromagnetic behaviour can be obtained also in overmoded reactors.

The experimental tests on the reactor were conducted in conditions similar to those considered in the numerical models. The reactor was loaded with the quartz sample holder, the Duraboard disc, and the Nicalon sample, as shown in Fig. 10. A microwave power of 1000 W in the heating stage, and of about 850 W in the infiltration stage, was delivered to the reactor by means of a single excitation channel. The level of the reflected power was determined with the help of a high-power circulator mounted just after the magnetron, which conveys the reflected power to a detector. The latter was calibrated short-circuiting the port of the circulator towards the reactor and varying the power emitted by the magnetron. By acting on the tuning stubs, the reflected power was kept close to the detection limit of the system throughout the infiltration process. The temperature of the sample was

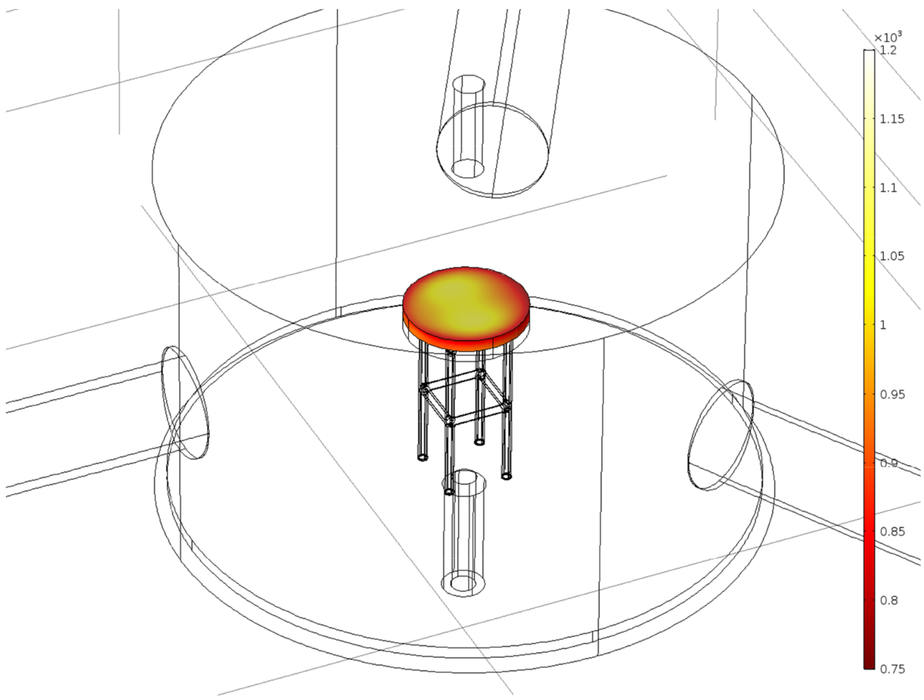

Fig. 10. Temperature distribution of the Nicalon sample, in the same configuration of Figs. 8 and 9, calculated with Comsol Multiphysics. In the modeling, the reactor is excited at 2.4763 GHz with a power of 1000 W, delivered through the excitation channel on the left of the figure. The initial temperature of the sample and of the reactor walls was fixed to 200 °C. The color legend on the right is in degrees K.

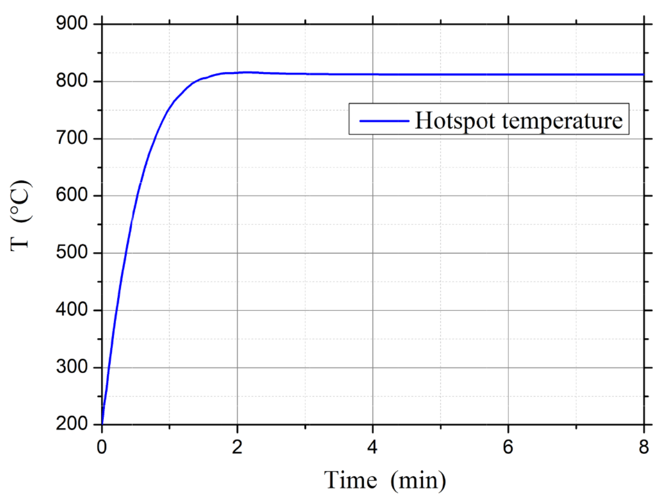

Fig. 11. Time dependence of the temperature of the hot spot of Fig. 10.

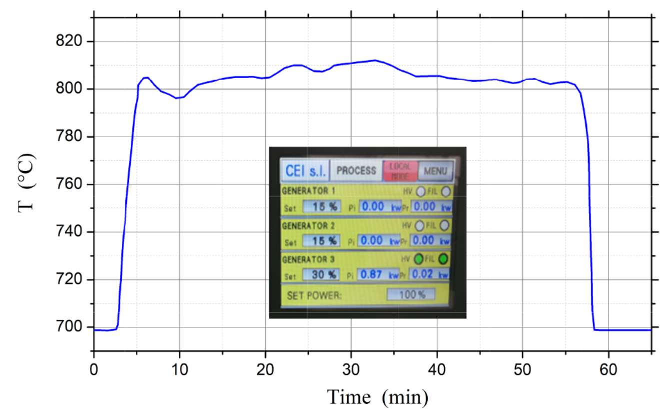

Fig. 12. Experimental Nicalon temperature during the heating and the infiltration process, determined in the central part of its upper surface. The lower limit in the temperature reading of the detector is 700 °C. The inset is a picture of the control panel of the magnetrons, reporting the typical incident (P_i) and reflected (P_r) power during the infiltration stage.

monitored by means of a digital pyrometer (Dias Pyrospot DSR 10NV), providing also its emissivity.

The evolution of the Nicalon temperature during the heating and the infiltration process is shown in Fig. 12. The inset shows the control panel of the magnetrons, indicating a typical incident power (P_i) and reflected power (P_r) during the infiltration stage.

In these tests, the temperature of the sample was brought from the initial value of 200 °C, achieved by means of the conventional resistive heating enabled by the reactor, to about 800 °C on the sample surface, exciting the reactor with 1000 W of MW power. The pre-heating of the reactor to 200 °C is usually done in order to remove the possible residual humidity, which would interfere with the chemical reaction (1). Taking account of the inverse temperature profile characteristics of the microwave heating, 800 °C on the sample surface corresponds to internal sample temperatures suited for the CVI process. Once this temperature was achieved, the microwave power was reduced to about 850 W and the reactant gases were made to flow in the reactor, so activating the infiltration process. In this stage, the total gas pressure was kept to 150 mbar. The infiltration shown in Fig. 12 lasted about 50 min. In this period, the microwave power was slightly adjusted in a manual way, together with the position of the tuning stubs, in order to keep the desired surface temperature and a nearly critical coupling condition.

According to Fig. 12, the heating of the sample from 700 °C to 800 °C took about 2.3 min, in good agreement with the data shown in Fig. 11, where the same temperature interval is covered in about 2.8 min. Starting from the initial temperature of 200 °C, the infiltration conditions are reached in about 5 min employing a microwave power of 1000 W. The very fast heating of the sample represents a striking difference with respect to conventional CVI processes, in which the entire reactor chamber must be brought to the infiltration temperature and the thermalization of the sample requires a much longer period.

It is worth noting that the good agreement between the above theoretical and experimental heating times indicates that the doubts raised in recent literature [20] about the possibility to predict and control the electromagnetic and thermal behaviour of overmoded reactors appear not justified, provided that great accuracy is dedicated to

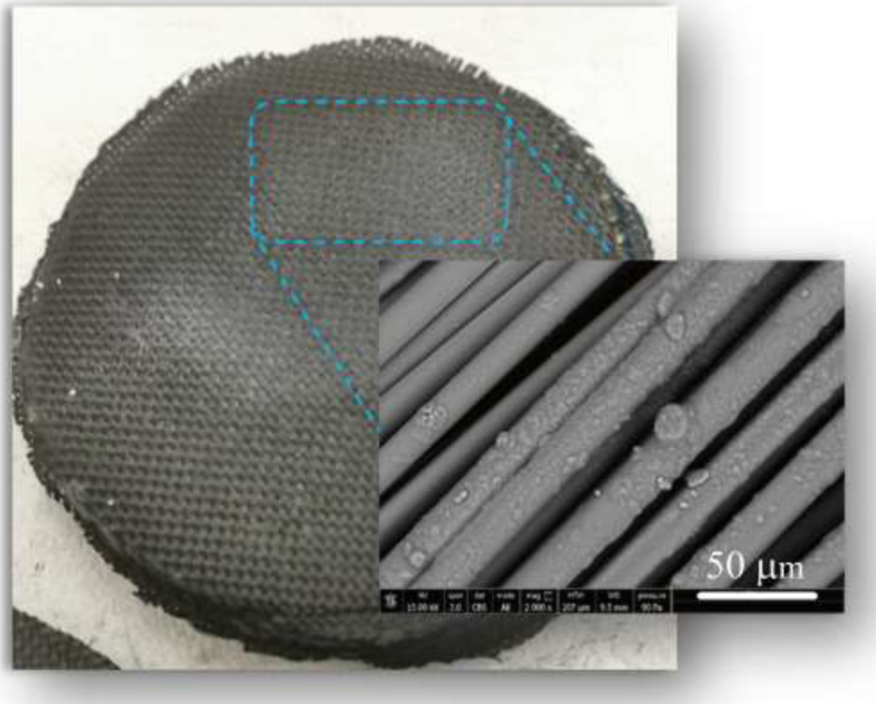

Fig. 13. Result of a typical MW-CVI process, with the SiC infiltrated on one of the central laminae of a multilayer Nicalon preform (lighter color regions). The inset reports an SEM image, showing the SiC grown on the preform fibers and among them.

the design of the reactor and to the characterization of the dielectric properties of the material to process.

The results of a typical infiltration process of the Nicalon sample are reported in Fig. 13, which shows the SiC grown on one of the central laminae of the multilayer preform, together with a scanning electron microscope (SEM) image of the most infiltrated region.

The analysis of the SiC infiltrated on the different laminae of the sample confirms the presence of a hotter region in the central part of the sample, in agreement with the temperature distribution shown in Fig. 10. Moreover, the decrease of the infiltrated SiC that is observed moving toward the most external laminae of the preform confirms the inverse temperature profile predicted by the modeling and expected, in general, in the microwave heating.

The SEM image shown in Fig. 13 evidences the binding among the preform fibers due to the infiltrated SiC. A further discussion of the microscopic details of the infiltrated sample is beyond the scope of this paper and will be presented elsewhere.

In the case of samples larger than those investigated in this work, better efficiencies are expected thanks to the most favorable ratio between the power dissipated in the sample and the power dissipated in the walls of the reactor cavity. On the other hand, the microwave heating of samples larger than the employed wavelength is prone to scarcely homogenous temperature distributions. This inhomogeneous heating is exacerbated when the dielectric losses increase with the temperature. Indeed, in this case a positive feedback mechanism is established, which can generate several hot spots. In the proposed reactor, the inhomogeneous microwave heating can be mitigated either by distributing the microwave power over the three excitation channels or by rotating the sample.

In general, the use of magnetron sources, characterized by a fixed-frequency emission, often dependent on the emitted power and on the ambient conditions, can represent a serious limitation in the achievement of the robust infiltration processing needed at industrial levels. In this respect, the passage to fully controllable solid-state sources represents an ineludible step in the implementation of well-controlled and reproducible processing, necessary for high production yield and quality. From the point of view of the design of overmoded reactors, the use of solid-state sources makes less stringent the condition of overlapping consecutive modes and the use of a frequency tuning element, which is beneficial both for the energy efficiency and for the ease of construction. Moreover, different resonance modes can be excited in a rapid sequence by means of tunable solid-state sources. In this manner, a more homogeneous microwave heating can be obtained.

The implementation of solid-state sources in the described MW-CVI reactor is the direction to which our current work is oriented.

4. Conclusions

In summary, an overmoded reactor cavity for MW-CVI of ceramic matrix composites at a pilot scale was designed, built in high-quality graphite, and tested. A two-step design was followed. First, the dimensions of the cavity were chosen on the basis of the spectral characteristics and of the expected energy efficiency, obtained by means of a general analysis. Then, a resonance mode enabling a high heating efficiency was identified through a rigorous modeling study. Experimental tests on the reactor loaded with different samples showed that the critical coupling can be reached in a large variety of conditions. In the case of low-density Nicalon preforms, the power dissipated in the sample is greater than 60% of the power coupled to the reactor, despite the aging of the cavity walls due to the many infiltration cycles. Thanks to this efficiency, typical SiC-fiber reinforced preforms having a volume of the order of 100 cm^3 can be heated up to about 900 °C in 5 min, using 1 kW of microwave power. The proposed design method, whose general approach is substantiated by a good agreement between calculated and observed quantities, is expected to become an important tool in the design of overmoded reactors for different applications.

Declaration of Competing Interest

The authors declare that they have no known competing financial interests or personal relationships that could have appeared to influence the work reported in this paper.

Acknowledgments

The economical support of the European Union Seventh Framework Programme (FP7/2007-2013), under the grant agreement no. 280464, is gratefully acknowledged. The authors also wish to acknowledge CISUP – Centre for Instrumentation Sharing – University of Pisa for the use of the FEI Quanta 450 ESEM FEG.

Appendix A. Supplementary data

Supplementary data to this article can be found online at https://doi.org/10.1016/j.cej.2020.126609.

References

[1] R. Meredith, Engineers' Handbook of Industrial Microwave Heating, IET, Stevenage, United Kingdom (1998). doi: 10.1049/PBPO025E.
[2] R.E. Collin, Foundations for Microwave Engineering, 2nd ed., Wiley-IEEE Press, 2001.
[3] E.T. Thostenson, T.-W. Chou, Microwave processing: fundamentals and applications, Compos. Part A: Appl. Sci. Manufacturing 30 (9) (1999) 1055–1071, https://doi.org/10.1016/S1359-835X(99)00020-2.
[4] R.R. Mishra, A.K. Sharma, Microwave–material interaction phenomena: heating mechanisms, challenges and opportunities in material processing, Compos. A Appl. Sci. Manuf. 81 (2016) 78–97, https://doi.org/10.1016/j.compositesa.2015.10.035.
[5] S. Das, A.K. Mukhopadhyay, S. Datta, D. Basu, Prospects of microwave processing: an overview, Bull. Mater. Sci. 32 (1) (2009) 1–13, https://doi.org/10.1007/s12034-009-0001-4.
[6] Y.V. Bykov, K.I. Rybakov, V.E. Semenov, High-temperature microwave processing of materials, J. Phys. D Appl. Phys. 34 (13) (2001) R55–R75, https://doi.org/10.1088/0022-3727/34/13/201.
[7] M. Oghbaei, O. Mirzaee, Microwave versus conventional sintering: a review of fundamentals, advantages and applications, J. Alloy. Compd. 494 (1-2) (2010) 175–189, https://doi.org/10.1016/j.jallcom.2010.01.068.
[8] R. Rosa, P. Veronesi, S. Han, V. Casalegno, M. Salvo, E. Colombini, C. Leonelli, M. Ferraris, Microwave assisted combustion synthesis in the system Ti–Si–C for the joining of SiC: experimental and numerical simulation results, J. Eur. Ceram. Soc. 33 (10) (2013) 1707–1719, https://doi.org/10.1016/j.jeurceramsoc.2013.03.005.
[9] D.A. Jones, T.P. Lelyveld, S.D. Mavrofidis, S.W. Kingman, N.J. Miles, Microwave heating applications in environmental engineering—a review, Resour. Conserv. Recycl. 34 (2) (2002) 75–90.
[10] F. Marken, Chemical and electro-chemical applications of in situ microwave heating, Annu. Reports Prog. Chem. – Sect. C. 104 (2008) 124–141, https://doi.org/10.1039/b703986g.
[11] S. Singh, D. Gupta, V. Jain, A.K. Sharma, Microwave processing of materials and applications in manufacturing industries: a review, Mater. Manuf. Processes 30 (1) (2015) 1–29, https://doi.org/10.1080/10426914.2014.952028.
[12] A. Lazzeri, CVI Processing of ceramic, Ceram. Compos. Process. Methods. John Wiley & Sons (2012) 313–349.
[13] I.M. Low, Advances in ceramic matrix composites: Introduction, Woodhead Publishing, 2018. doi: 10.1016/B978-0-08-102166-8.00001-3.
[14] W. Krenkel, Ceramic Matrix Composites: Fiber Reinforced Ceramics and Their Applications, John Wiley & Sons, 2008 doi: 10.1002/9783527622412.
[15] R. Naslain, Design, preparation and properties of non-oxide CMCs for application in engines and nuclear reactors: an overview, Compos. Sci. Technol. 64 (2) (2004) 155–170, https://doi.org/10.1016/S0266-3538(03)00230-6.
[16] D. Jaglin, J. Binner, B. Vaidhyanathan, C. Prentice, B. Shatwell, D. Grant, Microwave heated chemical vapor infiltration: Densification mechanism of SiCf/SiC composites, J. Am. Ceram. Soc. 89 (2006) 2710–2717. doi: 10.1111/j.1551-2916.2006.01127.x.
[17] A.C. Metaxas, R.J. Meredith, Industrial Microwave Heating, IET, London, United Kingdom, 2008.
[18] S.Y. Foong, R.K. Liew, Y. Yang, Y.W. Cheng, P.N.Y. Yek, W.A. Wan Mahari, X.Y. Lee, C.S. Han, D.-V. Vo, Q. Van Le, M. Aghbashlo, M. Tabatabaei, C. Sonne, W. Peng, S.S. Lam, Valorization of biomass waste to engineered activated biochar by microwave pyrolysis: progress, challenges, and future directions, Chem. Eng. J. 389 (2020) 124401, https://doi.org/10.1016/j.cej.2020.124401.
[19] J. Sun, W. Wang, Q. Yue, Review on microwave-matter interaction fundamentals and efficient microwave-associated heating strategies, Materials 9 (2016) 231. doi: 10.3390/ma9040231.
[20] G.S.J. Sturm, M.D. Verweij, A.I. Stankiewicz, G.D. Stefanidis, Microwaves and microreactors: design challenges and remedies, Chem. Eng. J. 243 (2014) 147–158, https://doi.org/10.1016/j.cej.2013.12.088.
[21] T. Mitani, N. Hasegawa, R. Nakajima, N. Shinohara, Y. Nozaki, T. Chikata, T. Watanabe, Development of a wideband microwave reactor with a coaxial cable structure, Chem. Eng. J. 299 (2016) 209–216, https://doi.org/10.1016/j.cej.2016.04.064.
[22] G. Annino, M. Cassettari, M. Fittipaldi, M. Martinelli, Complex response function of whispering gallery dielectric resonators, Int. J. Infrared Millimeter Waves 22 (2001) 1485–1494, https://doi.org/10.1023/A:1015038606997.
[23] G. Annino, M. Cassettari, M. Martinelli, Millimeter wave dielectric resonators, Recent Res. Dev. Microw. Theory & Tech., vol. 2, KERALA:Transworld Research Network, (2004) 195–236. ISBN: 81-7895-150-9.
[24] C.A. Balanis, Advanced Engineering Electromagnetics, 2nd ed., John Wiley & Sons, 2012.
[25] High-frequency ELectro-Magnetic technologies for advanced processing of ceramic matrix composites and graphite expansion" (HELM), FP7-NMP.2011.4.0-1, GA n°. 280464. http://www.helm-project.eu/.
[26] R. D'Ambrosio, L. Aliotta, V. Gigante, M.B. Coltelli, G. Annino, A. Lazzeri, Design of a pilot-scale microwave heated chemical vapor infiltration plant: An innovative approach, J. Eur. Ceram. Soc. (2020), https://doi.org/10.1016/j.jeurceramsoc.2020.05.073.
[27] H. Weyl, Über die Randwertaufgabe der Strahlungstheorie und asymptotische Spektralgesetze, J. Fur Die Reine Und Angew. Math. 143 (1913) 177–202, https://doi.org/10.1515/crll.1913.143.177.
[28] D.A. Hill, Electromagnetic Fields in Cavities: Deterministic and Statistical Theories, IEEE Press, New York, 2009. doi: 10.1002/9780470495056.
[29] J.F. Dawson, T. Konefal, M.P. Robinson, A.C. Marvin, S.J. Porter, L.C. Chirwa, Field statistics in an enclosure with an aperture effect of Q-factor and number of modes, IEEE Int. Symp. Electromagn. Compat. 1 (2005) 141–146, https://doi.org/10.1109/ISEMC.2005.1513489.
[30] D. Kajfez, P. Guillon, Dielectric Resonators, 2nd ed., Noble Publishing Corporation, Atlanta, 1998 doi: 1-884932-05-3.
[31] J.D. Jackson, Classical Electrodynamics, 2nd ed., John Wiley & Sons, New York, 1975.
[32] A. Cozza, The role of losses in the definition of the overmoded condition for reverberation chambers and their statistics, IEEE Trans. Electromagn. Compat. 53 (2) (2011) 296–307, https://doi.org/10.1109/TEMC.2010.2081993.
[33] L.R. Arnaut, G. Gradoni, Probability distribution of the quality factor of a mode-stirred reverberation chamber, IEEE Trans. Electromagn. Compat. 55 (1) (2013) 35–44, https://doi.org/10.1109/TEMC.2012.2213257.
[34] P. Hallbjorner, U. Carlberg, K. Madsen, J. Andersson, Extracting electrical material parameters of electrically large dielectric objects from reverberation chamber measurements of absorption cross section, IEEE Trans. Electromagn. Compat. 47 (2) (2005) 291–303, https://doi.org/10.1109/TEMC.2005.847391.
[35] O. Klein, S. Donovan, M. Dressel, G. Grüner, Microwave cavity perturbation technique: Part I: Principles, Int. J. Infrared Millimeter Waves 14 (1993) 2423–2457.
[36] G. Annino, A. Cintio, R. D'Ambrosio, A. Lazzeri, Dielectric characterization of Si, SiC, SiC/SiC and C/SiC samples, in: 17th Int. Conf. Microw. High-Frequency Heating, AMPERE 2019, 2019. http://ampere2019.com/program/topics/.
[37] Archer Technicoat Ltd. https://www.cvd.co.uk/.
[38] Schunk Carbon Technology. https://www.schunk-carbontechnology.com/.
[39] W.E. Courtney, Analysis and evaluation of a method of measuring the complex permittivity and permeability of microwave insulators, IEEE Trans. Microw. Theory Tech. 18 (1970) 476–485.
[40] Schunk Carbon Technology, private communication.
[41] COMSOL Multiphysics. https://www.comsol.it/.
[42] JKRIZAY: Custom quartz and alumina fabrication. http://www.jkrizay.com/.
[43] Unifrax. https://www.unifrax.com/.
[44] R.A. Waldron, The Theory of Waveguides and Cavities, Gordon and Breach Science Publishers, 1969.
[45] H.M. Altschuler, Dielectric Constant, in: E. M. Sucher and J. Fox (Ed.), Handb. Microw. Meas., Polytechnic Press of the Polytechnic Inst. Brooklyn, New York, 1963: pp. 518–548.
[46] G. Annino, M. Cassettari, I. Longo, M. Martinelli, Whispering Gallery Modes in a Dielectric Resonator: Characterization at Millimeter Wavelength, IEEE Trans. Microw. Theory Tech. 45 (1997) 2025–2034. doi: 10.1109/22.644226.